Ziegler–Natta Ethylene Insertion Reaction for a Five-Coordinate Titanium Chloride Complex Bridged to an Aluminum Hydride Cocatalyst

Vidar R. Jensen,*,† Knut J. Børve,† and Martin Ystenes§

Contribution from the Department of Chemistry, University of Bergen, Allégt. 41, N-5007 Bergen, Norway, and the Department of Inorganic Chemistry, The Norwegian Institute of Technology, N-7034 Trondheim, Norway

Received July 22, 1994®

Abstract: The Ziegler–Natta ethylene insertion into the metal–methyl bond in the neutral, bimetallic compound $AlH_2(\mu\text{-}Cl)_2TiCl_2(CH_3)$ has been studied with reaction path calculations and gradient geometry optimizations. No symmetry constraints have been imposed. The reaction path calculations and the geometry optimizations have been performed at the SCF level of theory using extended atomic basis sets. Correlation effects of all valence electrons have been included at the important stationary points on the potential energy surface (PES). A cut through the PES along the reaction path from the π complex to the propyl product for the direct insertion mechanism is presented in detail, as well as equilibrium structures of reactants and the transition state of ethylene π coordination. The system is seen to prefer geometries of C_s symmetry, and only departs from symmetry on short sections along the reaction path in order to relieve strain through rotations of the polymer chain. At the correlated level, the PES is almost flat along the reaction path until the transition state of ethylene insertion as determined at the SCF level of accuracy. Beyond this point, the energy decreases along the reaction path, resulting in an overall reaction enthalpy of 21.9 kcal/mol. The two bridging chlorides are found to behave dynamically, with an interchange in the bond distance asymmetry from the reactant to the product taking place synchronously with a polymer chain flipping due to the migratory insertion.

1. Introduction

Polymerization of olefins by Ziegler–Natta (ZN) catalysts is a remarkable reaction. It is extremely fast,[1–4] yields long molecular chains, and may proceed with a stereospecificity that is higher than for any other nonenzymatic reactions.[5] The mechanism by which the olefin is inserted has been the subject of numerous studies, and several reasonable mechanistic schemes have been suggested.[6–10] In the present paper, the Cossee mechanism[6] will be discussed. According to this mechanism, a propagation step is initiated by the coordination of the monomer onto a vacant site on a five-coordinate, square-pyramidal metal complex, with at least one alkyl ligand. The monomer subsequently inserts into the metal–alkyl bond via a four-center transition state involving the alkyl group, the alkene, and the transition metal.

A number of quantum chemical studies have been performed to evaluate the Cossee mechanism, most of which deal with models for metallocene catalysts. Experimental studies of catalysts for homogeneous polymerization of ethylene[11–13] have identified catalytic species as titanocene or zirconocene alkyl complexes of the type Cp_2MR^+. Ethylene coordination energies of 33–49 kcal/mol are calculated for the cationic models $[Cl_2M(CH_3)(C_2H_4)]^+$ (M = Ti, Zr)[14–18] where the chlorides are models for cyclopentadienyl ligands. Kawamura-Kuribayashi *et al.*[19] found an ethylene coordination energy of 33 kcal/mol for $[(SiH_2Cp_2)ZrCH_3(C_2H_4)]^+$. Cationic species also have a low barrier for the olefin insertion. Castonguay and Rappé[17] calculated the barrier for olefin insertion in $Cl_2ZrCH_3^+$ to be 9 kcal/mol below the reactant asymptote (infinite separation of reactants), while a much lower value, 27.5 kcal/mol, was reported in ref 19. Recent studies which include electron correlation in the geometry optimizations confirm that the potential energy surface (PES) of olefin coordination and insertion runs well below the reactant asymptote for the cationic metallocene systems.[20,21] In ref 20, the whole reaction proceeds downhill in energy without

† University of Bergen.
§ Norwegian Institute of Technology.
® Abstract published in *Advance ACS Abstracts*, March 15, 1995.

(1) Kaminsky, W.; Külper, K.; Niedobla, S. *Makromol. Chem. Macromol. Symp.* **1986**, *377*, 3. A turnover rate of 200 000 s^{-1} is reported.
(2) Soga, K.; Ohgizawa, M.; Shiono, T. *Makromol. Chem. Rapid Commun.* **1989**, *10*, 503.
(3) Kashiwa, N.; Yoshitake, J. *Makromol. Chem. Rapid Commun.* **1982**, *83*, 211.
(4) Keii, T.; Terano, M.; Kimura, K.; Ishii, K. *Makromol. Chem. Rapid Commun.* **1987**, *8*, 587.
(5) Pino, P.; Mülhaupt, R. In *Transition Metal Catalyzed Polymerizations*; Quirk, R., Ed.; Cambridge University Press: Cambridge, 1983; MMI Symposium Series. Vol. 4, p 23.
(6) Cossee, P. *J. Catal.* **1964**, *3*, 80.
(7) Ivin, K. J.; Rooney, J. J.; Stewart, C. D.; Green, M. L. H.; Mahtab, R. *J. Chem. Soc., Chem. Commun.* **1978**, 604.
(8) Brookhart, M.; Green, M. L. H. *J. Organomet. Chem.* **1983**, *250*, 395.
(9) Brookhart, M.; Green, M. L. H.; Pardy, R. B. A. *J. Chem. Soc., Chem. Commun.* **1983**, 691.
(10) Ystenes, M. *J. Catal.* **1991**, *129*, 383.
(11) Alelyunas, Y. W.; Jordan, R. F.; Echols, S. F.; Borkowsky, S. L.; Bradley, P. K. *Organometallics* **1991**, *10*, 1406.
(12) Eisch, J. J.; Caldwell, K. R.; Werner, S.; Krüger, C. *Organometallics* **1991**, *10*, 3417.
(13) Yang, X.; Stern, C. L.; Marks, T. J. *J. Am. Chem. Soc.* **1991**, *113*, 3623.
(14) Fujimoto, H.; Yamasaki, T.; Mizutani, H.; Koga, N. *J. Am. Chem. Soc.* **1985**, *107*, 6157.
(15) Jolly, C.; Marynick, D. S. *J. Am. Chem. Soc.* **1989**, *111*, 7968.
(16) Kawamura-Kuribayashi, H.; Koga, N.; Morokuma, K. *J. Am. Chem. Soc.* **1992**, *114*, 2359.
(17) Castonguay, L. A.; Rappé, A. K. *J. Am. Chem. Soc.* **1992**, *114*, 5832.
(18) Axe, F. U.; Coffin, J. M. *J. Phys. Chem.* **1994**, *98*, 2567.
(19) Kawamura-Kuribayashi, H.; Koga, N.; Morokuma, K. *J. Am. Chem. Soc.* **1992**, *114*, 8687.
(20) Weiss, H.; Ehrig, M.; Ahlrichs, R. *J. Am. Chem. Soc.* **1994**, *116*, 4919.
(21) Meier, R. J.; van Doremaele, G. H. J.; Iarlori, S.; Buda, F. *J. Am. Chem. Soc.* **1994**, *116*, 7274.

0002-7863/95/1517-4109$09.00/0

passing any stationary point, i.e., neither a π complex nor a transition state was found. However, there are indications[22] that calculations on free cationic species may exaggerate the strength of the ethylene coordination as well as underestimate the insertion barrier.

In the present paper, we have used a model system quite similar to the ones studied by Armstrong *et al.*[23] and Novaro *et al.*,[24,25] the neutral, bimetallic $AlH_2(\mu\text{-}Cl)_2TiCl_2(CH_3)$. This complex can be regarded as a contact ion pair including $Cl_2TiCH_3^+$, which is reported to promote ethylene insertion,[26] and $AlCl_2H_2^-$ as a model of the counterion. Eisch *et al.*[12] identified $AlCl_4^-$ as the cocatalyst counterion in an active ethylene polymerization catalyst. In this way, an overall neutral model has been constructed, which should overcome what appears to be shortcomings of the charged models.

Armstrong *et al.*[23] performed semiempirical (CNDO) calculations of the ethylene insertion into the $Ti-CH_3$ bond in $AlCl_2(\mu\text{-}Cl)_2TiCl_2(CH_3)$, and they concluded that the role of the aluminum moiety is to form the bridging that makes titanium adopt a high coordination number and thus a trigonal-bipyramidal or octahedral site symmetry, which is seen to give a labile Ti−alkyl bond and thus favors ethylene insertion. The initial olefin coordination was claimed to be the rate-determining step. In contrast, Novaro *et al.*,[24,25] modeling the olefin insertion in $Al(CH_3)_2(\mu\text{-}Cl)_2TiCl_2(CH_3)$ at the *ab initio* SCF level, found the transition state within the insertion step (~15 kcal/mol above the asymptote). The calculated barrier corresponds well to reported experimental barriers (6−12 kcal/mol[27−30]), but the overall energy (−40 kcal/mol) appears to be too large, as the experimental reaction enthalpy for addition of ethylene to alkanes larger than methane is −22.2 kcal/mol.[31] Experimental or assumed geometry parameters were used in refs 24 and 25, and electron correlation was not accounted for. In order to overcome the limitations of the methods used in refs 23−25 and still maintain the advantages of this type of model, we decided to calculate the ZN ethylene insertion into the titanium−methyl bond in $AlH_2(\mu\text{-}Cl)_2TiCl_2(CH_3)$ using gradient methods accounting for relaxation throughout the reaction. Previous calculations on smaller models also show that inclusion of electron correlation effects is important for predicting reliable energy differences for the insertion reaction.[22,32,33] High-level treatment of electron correlation was therefore included in the present work.

Our main aim is therefore to provide detailed information about structures and energetics of the insertion step according to the Cossee mechanism and, in particular, to investigate the role of the cocatalyst counterion in the homogeneous ZN process. An important feature is that the present PES is expected to be an upper bound to the energy along the reaction path from the reactants to the transition state. This follows from the minimal separation of the ion pair, making the charge-induced dipole force operating on the incoming ethylene molecule the weakest possible. Taken together with results from accurate calculations on cationic models of related systems,[14−17,19,20] the present PES should bracket the energy profile of the insertion step with respect to the ion pair association. The calculations address a specific homogeneous system, and keeping in mind the complexity and diversity of the field of ZN catalysis, one should be careful when transferring our findings to other ZN catalysts. However, there are obvious similarities between the present model and models postulated for the active center in heterogeneous catalysts.[6,10,34] These include a coordination number of six (with a bound monomer), chloride ligands, and bridges to a main group metal. It therefore appears likely that the present work also should provide some insight into the function of halide-based heterogeneous catalysts.

2. Computational Details

2.1. Reaction Pathway Calculations. The self-consistent field (SCF) approximation was used in all analytic gradient geometry optimizations, saddle point localizations, and reaction path calculations. In all the SCF calculations, titanium was described by Wachters primitive basis[35] contracted to [10s, 8p, 3d] with the standard modifications as implemented in GAMESS.[36] The most diffuse s function was removed and replaced by one s function spanning the 3s−4s region ($\alpha_s = 0.209$). Two p functions to describe the 4p region were added ($\alpha_p = 0.156, 0.0611$), and one diffuse d-primitive was added ($\alpha_d = 0.0743$). Chlorine and aluminum were described by effective core potentials (ECPs) according to Hay and Wadt.[37] The valence basis sets were double-ζ in the 3s and 3p region. For chlorine, a d function with exponent 0.75 was also included in the valence basis set. Hydrogen and carbon were described by 6-31G(d) basis sets.[38,39] For carbon, the d function exponent was 0.8. For the reaction path calculations and geometry optimizations, the GAMESS set of programs[36] was used, and the calculations were performed on the Intel Paragon XP/S at the National Massive Parallel Processing center, University of Bergen, and on the Intel Paragon A/4 at SINTEF, Trondheim.

The reaction pathway calculations were carried out by first locating the transition states and then integrating the intrinsic reaction coordinate (IRC) equation[40] in both forward and backward directions, using the Gonzales and Schlegel second-order method.[41,42] The step size used was 0.3 amu$^{1/2}$ bohr. The true IRC is defined as the minimum energy path connecting the reactants to products via the transition state. The IRC follows the gradient from a saddle point; thus, it is not possible to break symmetry. This is of direct relevance to the present system, since the transition state of ethylene insertion is determined to be of C_s symmetry, whereas rotations to relieve strain in the polymer chain destroy the plane of symmetry. Hence, the present reaction offers several examples of bifurcations.[43] The path of steepest descent will follow a ridge after passing through a valley−ridge inflection point (VRI), whereas a useful chemical reaction path should follow the valleys. If a small displacement from perfect C_s symmetry is made,

(22) Jensen, V. R.; Siegbahn, P. E. M. *Chem. Phys. Lett.* **1993**, *212*, 353.
(23) Armstrong, D. R.; Perkins, P. G.; Stewart, J. J. P. *J. Chem. Soc., Dalton Trans.* **1972**, 1972.
(24) Giunchi, G.; Clementi, E.; Ruiz-Vizcaya, M. E.; Novaro, O. *Chem. Phys. Lett.* **1977**, *49*, 8.
(25) Novaro, O.; Blaisten-Barojas, E.; Clementi, E.; Giunchi, G.; Ruiz-Vizcaya, M. E. *J. Chem. Phys.* **1978**, *68*, 2337.
(26) Uppal, J. S.; Johnson, D. E.; Staley, R. H. *J. Am. Chem. Soc.* **1981**, *103*, 508.
(27) Natta, G.; Pasquon, I. *Adv. Catal.* **1959**, *11*, 1.
(28) Chien, J. C. W. *J. Am. Chem. Soc.* **1959**, *81*, 86.
(29) Machon, J.; Hermant, R.; Hoteaux, J. P. *J. Polym. Sci. Symp.* **1975**, *52*, 107.
(30) Chien, J. C. W.; Razavi, A. *J. Polym. Sci., Part A: Polym. Chem.* **1988**, *26*, 2369.
(31) Aylward, G. H.; Findlay, T. J. V. *SI Chemical Data*, 2nd ed.; John Wiley and Sons: Hong Kong, 1985.
(32) Siegbahn, P. E. M. *Chem. Phys. Lett.* **1993**, *205*, 290.
(33) Siegbahn, P. E. M. *J. Am. Chem. Soc.* **1993**, *115*, 5803.
(34) Corradini, P.; Busico, V.; Guerra, G. In *Transition Metals and Organometallics as Catalysts for Olefin Polymerization*; Kaminsky, W., Sinn, H., Eds.; Springer Verlag: Berlin, Heidelberg, 1988; p 337.
(35) Wachters, A. J. H. *J. Chem. Phys.* **1970**, *52*, 1033.
(36) Schmidt, M. W.; Baldridge, K. K.; Jensen, J. H.; Koseki, S.; Gordon, M. S.; Nguyen, K. A.; Windus, T. L.; Elbert, S. T. *Quantum Chem. Program Exch. Bull.* **1990**, *10*, 52.
(37) Hay, P. J.; Wadt, W. R. *J. Chem. Phys.* **1985**, *82*, 284.
(38) Ditchfield, R.; Hehre, W. J.; Pople, J. A. *J. Chem. Phys.* **1971**, *54*, 724.
(39) Hehre, W. J.; Ditchfield, R.; Pople, J. A. *J. Chem. Phys.* **1972**, *56*, 2257.
(40) Fukui, K. *Acc. Chem. Res.* **1981**, *14*, 363.
(41) Gonzales, C.; Schlegel, H. B. *J. Phys. Chem.* **1990**, *94*, 5523.
(42) Gonzales, C.; Schlegel, H. B. *J. Chem. Phys.* **1991**, *95*, 5853.
(43) Valtazanos, P.; Ruedenberg, K. *Theor. Chim. Acta* **1986**, *69*, 281.

the path will generally follow the ridge for some distance after the VRI point and then diverge down to one of the valleys.[44]

To allow for following a valley after passing the present bifurcating regions, a distortion from the symmetric transition state of ethylene insertion was performed. The starting point of the reaction path calculations was then the located saddle point with the in-plane methyl hydrogen distorted 10^{-10} Å along the normal of the symmetry plane. In the present work, this point satisfies the criterion (maximum gradient below 10^{-4} hartree/bohr) for a converged geomtry optimization within C_1 symmetry. Since the located reaction path is slightly off the C_s transition point, the path is not unique and not the true IRC and should rather be referred to as a "meta-IRC" according to Fukui.[40]

A second transition state (C_1), caused by a rotation of the terminal ethyl group at the end of the insertion process, was also located. This transition state was used as a starting point of an IRC that connects the first path (described above) with the propyl product.

2.2. Energy Evaluations. In all the reported correlated calculations, extended atomic basis sets were used in a generalized contraction scheme,[45,46] and all valence electrons except those of 3s on chlorine were correlated. Relativistic effects were accounted for by first-order perturbation theory including the mass–velocity and Darwin terms.[47,48]

For Ti, Wachters primitive basis[35] was extended by adding one diffuse d function (α_d = 0.0720), two p functions (α_p = 0.15234, 0.05108), and three f functions (α_f = 1.3935308, 0.4997522, 0.2139998). The resulting primitive (14s, 11p, 6d, 3f) basis was contracted to [5s, 4p, 3d, 1f]. For chlorine, the Huzinaga primitive basis[49] was augmented by one diffuse p function (α_p = 0.044) and one d function (α_d = 0.55), leading to a contraction of (12s, 10p, 1d) to [4s, 4p, 1d]. For carbon, the primitive (9s, 5p) basis of Huzinaga[49] was extended with one d function (α_d = 0.63) and contracted to [3s, 2p, 1d]. For aluminum, the Huzinaga[50] primitive (12s, 9p) basis was used and contracted to [4s, 3p]. Hydrogen was described by the Huzinaga primitive (4s) basis[51] and contracted to [2s], with the exponents scaled by a factor of 1.2.

The correlated calculations were all performed using the modified coupled-pair function (MCPF) method,[52] which is a size-consistent, single-reference state method. The zeroth-order wave functions were defined at the SCF level. The core orbitals as well as 3s on chlorine were localized using an $\langle r^2 \rangle$ minimization procedure prior to the correlation treatment.[53] For the correlated calculations, the STOCKHOLM set of programs was used[54] and the calculations were performed on a cluster of IBM RS/6000 workstations at the University of Bergen.

Siegbahn *et al.*[55] recently pointed out that, using well-balanced basis sets of the double-ζ plus polarization type and a correlation treatment at the present level of sophistication, about 80% of the correlation effects on bond energies should normally be obtained. Similar estimates of the total correlation effects have earlier been obtained by others, see, e.g., Gordon and Truhlar.[56] An improved estimate of relative energies is thus obtained by simply adding 25% of the calculated correlation energy to the MCPF energy. This amounts to adding 20% of the difference between the SCF energy and the total extrapolated energy. The strategy is referred to as the parameterized CI-80 (PCI-80) method,[55] which has been adopted in all energy evaluations. In the present work, titanium, all the nearest neighbors of titanium, and all atoms involved in bond forming and breaking have been described by exactly the same type of basis sets as used in ref 55. Slightly smaller basis sets, without polarization functions, have been applied in the more remote and inert parts of the system, but this should not influence the results in any significant way.

The largest remaining error in our calculations is probably the incompleteness of the one-particle bases. Energetically, the present reaction is dominated by the breaking of the π bond in ethylene and the formation of a C–C single bond. It is well known that the Hartree–Fock (HF) limit corrections are larger for double bonds than single bonds.[57] In order to obtain energy differences of high accuracy, an estimate of the HF limit correction has been added to the PCI-80 energies to give the "best estimates" in Table 3. Preliminary studies of several different reactions involving π bond breaking in ethylene[58] indicate that the contribution from a HF limit correction to the present overall reaction energy should be a stabilizing of the reactants by 3–4 kcal/mol compared to the propyl product. In the present estimate of the overall reaction enthalpy for ethylene insertion, a value of 3.5 kcal/mol has been used. At the transition state, the C–C bond length in the ethylene moiety is intermediate between the corresponding equilibria bond lengths in ethylene and ethane. Accordingly, the energy of the reactants has been lowered by half of this correction (1.75 kcal/mol) compared to the transition state. Since the elongation of the C–C bond in ethylene is very small upon coordination, HF limit corrections for these structures are added as for reactants.

Zero-point vibrational corrections were obtained from SCF calculations (basis sets and program as for the geometry optimizations) of the frequencies within the harmonic approximation, and with the corrections scaled by 0.90. Temperature corrections of the enthalpies (298 K) were added as described by Hehre *et al.*[59] These corrections are included, along with the PCI-80 energies and HF limit corrections, to form the "best estimates" of the enthalpies in Table 3.

3. Results and Discussion

In the first part of this section, the reaction coordinate for the reaction under discussion is presented in terms of geometrical parameters, with special attention paid to the stationary points. In the second part, the potential energy curve along the reaction coordinate is presented, and energy differences, in particular the reaction barriers, are reported as calculated at various levels of theory.

3.1. The Reaction Pathway. The most important features of a given reaction are described by the stationary points of the associated potential energy surface (PES). For the investigated reaction, the direct ethylene insertion into the titanium–methyl bond in $AlH_2(\mu\text{-}Cl)_2TiCl_2(CH_3)$, seven stationary points, four minima and three saddle points, were located on the PES. No symmetry constraints were imposed during these geometry optimizations. Five of the stationary points, all possessing C_s symmetry, were believed to be important for the reaction, and correlation effects were thus accounted for at these geometries. The important stationary points are shown in Figure 1: the reactants (**1**), the transition state of ethylene π coordination (**2**), the π complex (**3**), the transition state of ethylene insertion (**4**), and the propyl product (**5**). In addition, two stationary points, a local minimum (structure **f** in Figure 2) and a transition state, were found on the reaction path, not far from the propyl product. These latter two stationary points, both possessing C_1 symmetry, are caused by rotation of the terminal ethyl group. A few other stationary points were located, but the ones presented in this paper are those which were found to have the lowest energy in their respective regions of the PES.

To ensure that the located transition structures connect the minima, reaction path calculations were performed. A second motive for performing these calculations was to obtain more detailed information about the reaction mechanism. The long

(44) Schlegel, H. B. *J. Chem. Soc., Faraday Trans.* **1994**, *90*, 1569.
(45) Almlöf, J.; Taylor, P. R. *J. Chem. Phys.* **1987**, *86*, 4070.
(46) Raffenetti, R. C. *J. Chem. Phys.* **1973**, *58*, 4452.
(47) Martin, R. L. *J. Chem. Phys.* **1983**, *87*, 750.
(48) Cowan, R. D.; Griffin, D. C. *J. Opt. Soc. Am.* **1976**, *66*, 1010.
(49) Huzinaga, S. *Approximate atomic functions II.* Report, Department of Chemistry, University of Alberta, 1971.
(50) Huzinaga, S. *J. Chem. Phys.* **1977**, *66*, 4245.
(51) Huzinaga, S. *J. Chem. Phys.* **1965**, *42*, 1293.
(52) Chong, D. P.; Langhoff, S. R. *J. Chem. Phys.* **1986**, *84*, 5606.
(53) Pettersson, L. G. M.; Åkeby, H. *J. Chem. Phys.* **1991**, *94*, 2968.
(54) STOCKHOLM is a general purpose quantum chemical set of programs written by P. E. M. Siegbahn, M. R. A. Blomberg, L. G. M. Pettersson, B. O. Roos, and J. Almlöf.
(55) Siegbahn, P. E. M.; Blomberg, M. R. A.; Svensson, M. *Chem. Phys. Lett.* **1994**, *223*, 35.
(56) Gordon, M. S.; Truhlar, D. G. *J. Am. Chem. Soc.* **1986**, *108*, 5412.
(57) Langhoff, S. R.; Bauschlicher, C. W., Jr.; Taylor, P. R. *Chem. Phys. Lett.* **1991**, *180*, 88.
(58) Børve, K. J.; Jensen, V. R. In progress.
(59) Hehre, W. J.; Radom, L.; Schleyer, P. v. R.; Pople, J. A. *Ab initio molecular orbital theory*; John Wiley and Sons: New York, 1986.

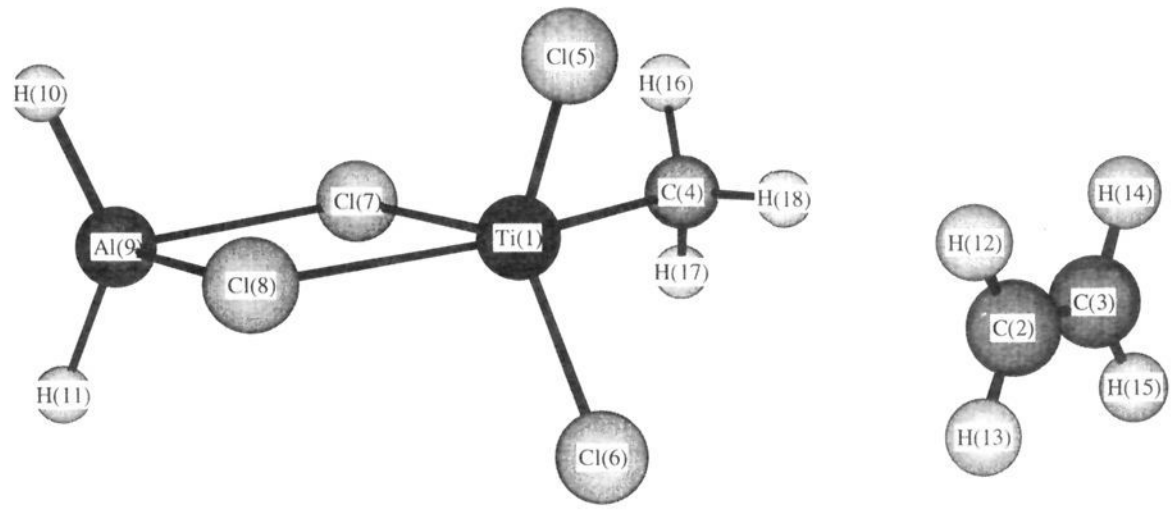

1

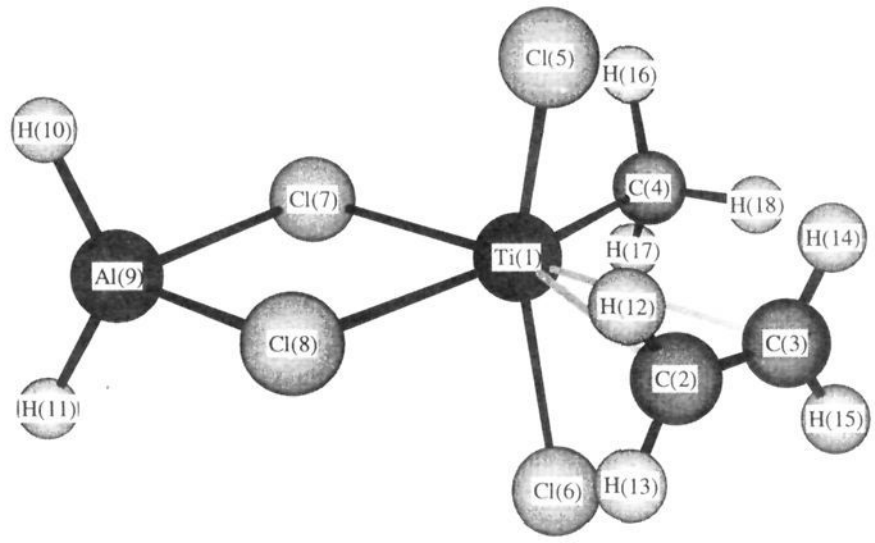

2, 3

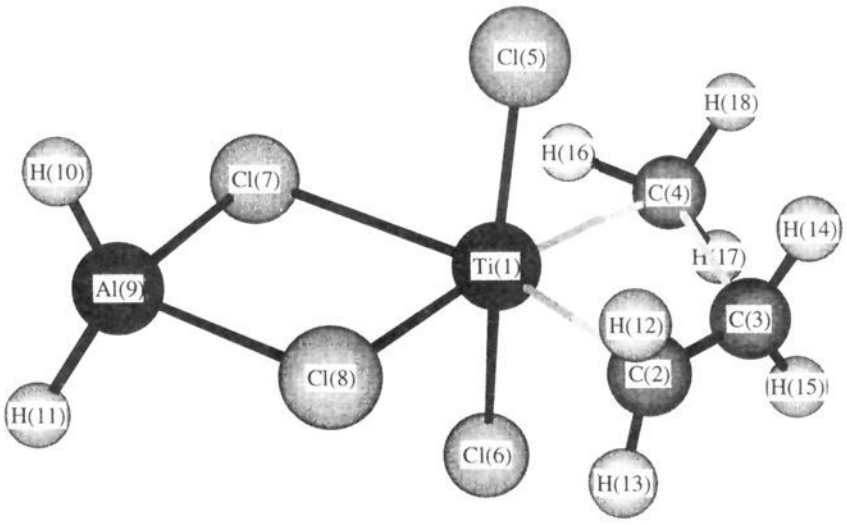

4

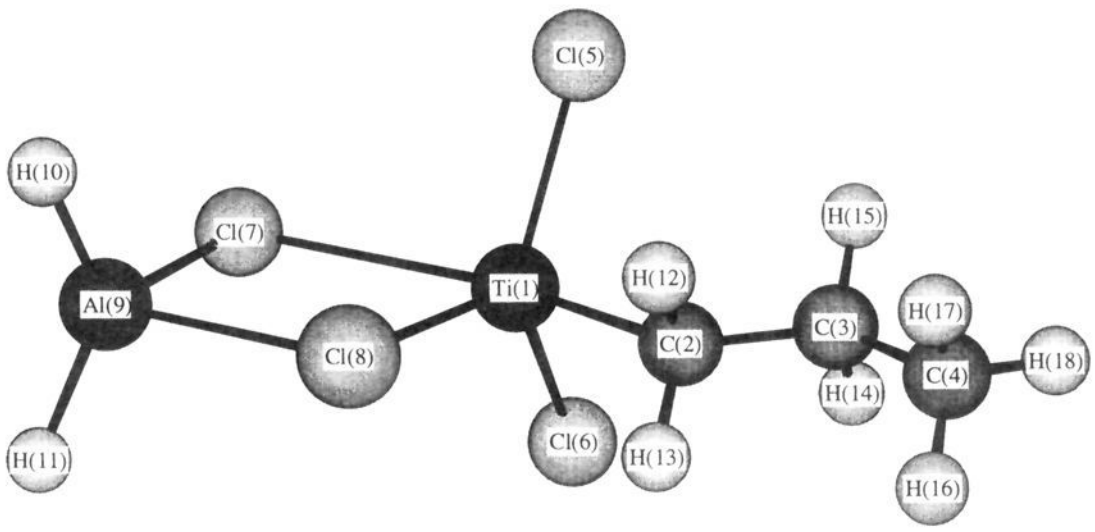

5

Figure 1. Important stationary points, all possessing C_s symmetry, found along the reaction path. Geometry parameters are listed in Table 1. The structures are: the reactants (**1**); the transition state of ethylene π coordination and the π complex (**2** and **3**, very similar structures); the transition state of ethylene insertion (**4**); and finally, the propyl product (**5**).

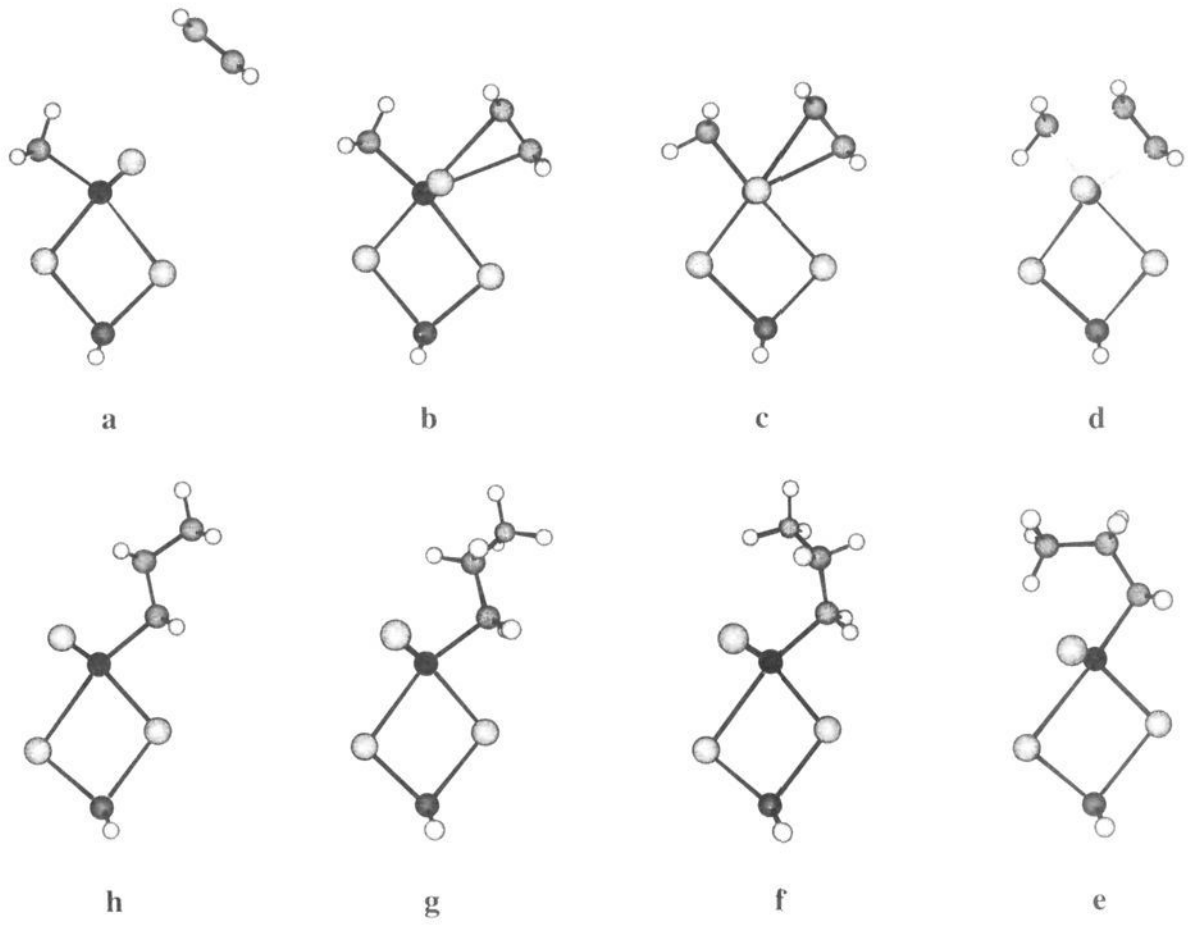

Figure 2. Top view of selected structures along the reaction path. The paper plane is the plane of symmetry, which is present in **a**, **b**, **d**, and **h**. The structures are the reactants, **a**; the π complex which is the starting point in the reaction pathway calculations (path coordinate 0), **b**; approaching the transition state with eclipsed methyl (path coordinate 0.13), **c**; the transition state of ethylene insertion (path coordinate 0.22), **d**; early during the first rotation in the propyl group (path coordinate 0.40); **e**; local minimum during the second rotation in the propyl group (path coordinate 0.70), **f**; last part of the second rotation in the propyl group (path coordinate 0.90), **g**; the propyl product (path coordinate 1.0), **h**.

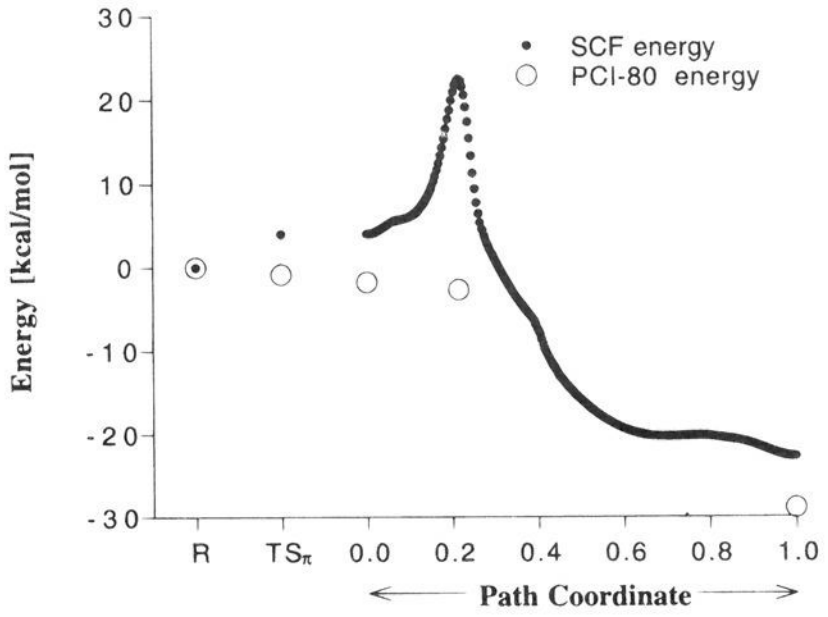

Figure 3. Energy as a function of the path coordinate from the π complex to the product. The total path length is 71.53 amu$^{1/2}$ bohr, and the path coordinate is the fraction of the total length. The energy is also shown for the reactants (R) and the transition state of the π complexation (TS_π). The latter two points, shown on the left side of the figure, were not included in the reaction path calculations.

section of the reaction path between the transition state of insertion and the final product was deemed to be of particular interest, as a possible polymer chain flipping should occur on this part of the PES. The reaction path calculations included 264 points on the potential energy surface with a total path length of 71.53 amu$^{1/2}$ bohr and connected the ethylene π complex to the propyl product. The SCF and PCI-80 energies as a function of the path coordinate (the fraction of the total path length) for the investigated reaction are shown in Figure 3.

In the reactant, titanium has an almost trigonal-bipyramidal configuration, structure **1**, the three chlorides Cl(5,6,7) being equatorial and the methyl group and Cl(8) being axial. Placing the methyl group in an equatorial position, by substituting one of the terminal chlorides, gives a slightly higher energy (~0.02 kcal/mol at the SCF level). The asymmetry in the bridging bonds is due to the *trans* influence from the axially bound methyl group. Cl(7) has no diagonally bound ligand and thus has a shorter bond toward titanium, as seen from the bond distances in Table 1 and as reflected in the overlap populations in Table 2. The difference in the Ti(1)–Cl(7,8) bond lengths also has a strong influence on the respective Al–Cl bonds. Within a bridge, a short Ti–Cl bond gives a long Al–Cl bond, and this tendency is seen throughout the structures **1**–**5**.

No reaction path calculations were performed to connect the stationary points related to the π coordination of ethylene, and this part of the reaction pathway is believed to consist of a simple translation of ethylene toward the metal within the plane of symmetry. The imaginary mode at the transition state of coordination, 48i cm^{-1}, has a dominating component along this direction. The angle $\angle$Cl(8)Ti(1)C(4) increases (162.6–169.5°) during coordination, giving a larger *trans* influence from C(4). Thus, the difference in the bridging bond distances increases during ethylene coordination with a weakening of the bridging Ti(1)–Cl(8) bond. Ethylene is very weakly bound in the π complex and is not seen to influence the bridging Ti(1)–Cl(7) bond notably. The weak π complexation in turn is demonstrated by the almost constant C–C distance in ethylene, 1.32–1.33 Å, during coordination. In fact, at the SCF level of theory, the ethylene π complex is not favored energetically relative to the reactants, as can be seen from the energy differences in Table 3. When correlation effects are included, a bond, although weak, exists between ethylene and the metal. Despite the fact that the SCF method does not treat the correlation effects which are present in reactions with transition metals, the SCF geometries are expected to be of sufficient quality for the energy evaluations used in the present work, as will be discussed later in this section.

Starting from the π complex, the methyl group rotates 60°, from **b** to **c**, to become eclipsed to the ethylene CH_2. A shoulder

Table 1. Selected Geometry Parameters for the Reactants (**1**), the Transition State of the π Complexation (**2**), the π Complex (**3**), the Transition State (**4**), and the Product (**5**), of Ethylene Insertion[a]

	structures				
parameter	**1**	**2**	**3**	**4**	**5**
Ti(1)−C(2)		3.20	3.05	2.18	2.05
Ti(1)−C(3)		3.22	3.05	2.50	3.06
Ti(1)−(C4)	2.04	2.04	2.04	2.17	4.43
Ti(1)−H(16)	2.60	2.60	2.60	2.07	4.73
Ti(1)−H(17)	2.60	2.60	2.60	2.89	4.73
Ti(1)−H(18)	2.57	2.55	2.55	2.89	5.22
C(2)−C(3)	1.32	1.33	1.33	1.40	1.53
C(3)−C(4)		3.85	3.69	2.16	1.53
C(2)−H(12,13)	1.08	1.08	1.08	1.08	1.09
C(3)−H(14,15)	1.08	1.08	1.08	1.07	1.08
C(4)−H(16)	1.08	1.08	1.08	1.11	1.09
C(4)−H(17)	1.08	1.08	1.08	1.08	1.09
C(4)−H(18)	1.08	1.09	1.09	1.08	1.09
Ti(1)−Cl(5,6)	2.22	2.27	2.28	2.32	2.23
Ti(1)−Cl(7)	2.43	2.38	2.39	2.60	2.85
Ti(1)−Cl(8)	2.74	2.86	2.86	2.57	2.41
Cl(7)−Al(9)	2.50	2.54	2.53	2.37	2.28
Cl(8)−Al(9)	2.32	2.29	2.29	2.38	2.54
Al(9)−H(10,11)	1.58	1.58	1.58	1.58	1.58
∠Ti(1)C(2)H(12,13)		98.0	97.4	104.3	103.2
∠Ti(1)C(3)H(14,15)		97.8	98.0	114.2	89.3
∠Ti(1)C(4)H(16)	108.8	109.0	109.0	70.0	99.4
∠Ti(1)C(4)H(17)	108.8	109.0	109.0	122.4	99.4
∠Ti(1)C(4)H(18)	106.7	105.2	105.3	122.4	132.3
∠Cl(7)Ti(1)C(2)		153.8	153.3	159.8	164.4
∠Cl(8)Ti(1)C(2)		74.8	74.4	80.0	87.5
∠Cl(8)Ti(1)C(4)	162.6	169.9	169.5	168.5	103.0
∠Ti(1)C(2)C(3)		77.3	77.3	85.6	117.2
∠C(2)C(3)C(4)		109.2	110.8	115.4	110.8
∠C(3)C(4)H(16)		124.0	124.0	140.6	111.3
∠C(3)C(4)H(17)		124.0	124.0	93.9	111.3
∠C(3)C(4)H(18)		48.6	49.6	93.9	110.3
∠H(12)C(2)H(13)	116.4	116.9	117.0	116.8	108.3
∠H(14)C(3)H(15)	116.4	117.2	117.3	116.9	107.2
∠H(16)C(4)H(17)	110.8	111.8	111.8	107.0	108.0
∠Cl(5)Ti(1)Cl(6)	116.2	153.5	157.5	170.9	117.7
∠Cl(7)Ti(1)Cl(8)	77.6	79.0	78.9	79.8	76.9
∠Cl(7)Al(9)Cl(8)	85.0	87.9	88.2	88.5	86.0
∠H(10)Al(9)H(11)	129.5	128.7	128.5	127.5	128.8
∠Cl(5)Ti(1)Cl(6)Cl(7)	173.0	165.2	164.0	−84.9	−92.0

[a] Units: bond distances, Å; angles, deg.

Table 2. Selected Overlap Populations [*e*] for the Reactants (**1**), the Transition State of the π Complexation (**2**), the π Complex (**3**), the Transition State (**4**), and the Product (**5**) of Ethylene Insertion

complex	Ti(1)−Cl(5)	Ti(1)−Cl(7)	Ti(1)−Cl(8)	Ti−C(2)	Ti−C(4)
1	0.76	0.38	0.22	−	0.51
2	0.74	0.40	0.13	0.03	0.47
3	0.75	0.39	0.13	0.04	0.46
4	0.78	0.21	0.24	0.23	0.30
5	0.76	0.18	0.40	0.48	−0.02

can be seen in the energy curve in Figure 3 at the end point of this rotation (path coordinate ~0.08). The methyl rotation also opens up the possibility of an α C−H agostic interaction which stabilizes the structure near the transition state. At the transition state of ethylene insertion (**c**), titanium has an almost square-bipyramidal configuration, with the two terminal chlorides located in axial positions. The imaginary frequency (433i cm^{-1}) is dominated by the C(3)−C(4) stretching mode. The two Ti−C distances are very similar, as are the two Ti−Cl−Al bridges. This is reflected in the overlap populations (Table 2) of the four equatorial bonds around titanium, which differ by no more than 0.09 *e*. During ethylene coordination and toward the transition state of insertion, the angle ∠Cl(5)Ti(1)Cl(6) increases strongly (116.2−170.9°). The *trans* influence from the opposite terminal chloride thus seems to be the reason for

Table 3. Energies and Enthalpies [kcal/mol] for the Transition State of π Complexation (**2**), the π Complex (**3**), the Transition State (**4**), and the Product (**5**) of Ethylene Insertion[a]

					best estimates		
species	ΔE_{SCF1}[b]	ΔE_{SCF2}[c]	ΔE_{MCPF}	ΔE_{PCI-80}	ΔE[d]	ΔH[e]	expt
2	+4.0	+6.1	+0.5	−0.9	−0.9	−0.1	
3	+3.9	+6.2	−0.2	−1.8	−1.8	−0.3	
4	+22.5	+23.7	+2.6	−2.7	−1.0	+0.9	+6−12[f]
5	−22.7	−22.4	−27.6	−28.9	−25.4	−21.9	−22.2[g]

[a] The energies and enthalpies are given relative to the reactants. [b] ΔE_{SCF1} refers to the HF/ECP results from the geometry optimizations. [c] The energies given as ΔE_{SCF2} were calculated using all-electron HF theory including relativistic effects. The wave functions from these calculations were used as zeroth-order wave functions in the correlated calculations. [d] HF limit corrections have been added to the PCI-80 energies, cf. the Computational Details section. [e] Enthalpies at 298 K. Zero-point vibrational corrections and temperature corrections have been added to the best estimates of ΔE, cf. the Computational Details section. [f] Activation energy measurements taken from refs 27−30. [g] Reaction enthalpy for addition of ethylene to alkanes larger than methane, in gas phase, 298 K.[31]

the longer Ti(1)−Cl(5,6) distances (2.22−2.32 Å) in the π complex and transition state of ethylene insertion as compared to the reactant.

At the transition state (structure **4**, Figure 1), the agostic interaction of the in-plane methyl hydrogen is quite evident, with C−H and Ti−H distances of 1.11 and 2.07 Å, respectively. α agostic interaction has earlier been suggested to be of importance during the chain propagation.[8,9] Similar evidence of α C−H agostic interaction at the transition state of ethylene insertion has been reported by Fujimoto *et al.*[14] and by Kawamura-Kuribayashi *et al.*[16] In ref 16 it is also claimed that this agostic interaction is the reason why the methyl group prefers to be eclipsed at the transition state. With the methyl staggered to the ethylene CH_2, the energy was significantly higher (~6 kcal/mol) and the vibrational analysis also revealed an additional imaginary frequency (303i cm^{-1}) due to rotation of the methyl group. This is mainly due to steric hindrance from the two terminal chlorides, which prohibits α agostic interaction with the staggered methyl conformation. This steric hindrance is also the reason why C_s symmetry is maintained along much of the reaction path. The system only departs from C_s symmetry on two limited sections along the reaction path. These two parts involve rotations of the growing polymer chain, and the rotations are made between structures possessing C_s symmetry.

After the transition state of ethylene insertion, the Ti(1)−C(4) distance increases strongly as the tail of the propyl group is moving away from titanium. However, during the first part of this process, a certain degree of α agostic interaction is maintained through a decreasing angle ∠Ti(1)C(4)H(16). When the Ti(1)−C(4) distance has increased to 3.04 Å, at a Ti(1)−H(16) distance of 2.40 Å, the propyl group starts the internal rotations to relieve the strain resulting from two eclipsed conformations. The starting point of the rotations can be discerned as a shoulder on the energy curve in Figure 3 (path coordinate ~0.40). First, the terminal methyl group rotates around the C(3)−C(4) bond to become staggered to the neighboring CH_2 (structure **e**, Figure 2). Then a 180° rotation of the terminal ethyl group around the C(2)−C(3) bond takes place (**f** and **g**). The two rotations are made in opposite directions, and when the final product is reached, the in-plane methyl hydrogen in the reactant has become the in-plane propyl hydrogen (H(18), Figure 1). After approximately 54° of the second rotation, a local minimum (**f**) is passed as the two CH_2 groups are in a staggered conformation. An eclipsed structure, after approximately 108° of rotation, is the last transition state

found on the reaction path. Structure **g** is located shortly after this transition state and, thus, not very far from the end point of the rotation, namely the propyl product (**h**). The propyl product (**5**, Figure 1) has a structure similar to the reactant, except that Cl(7) now is the axial chloride and bound *trans* to the propyl group, i.e., a flipping of the growing polymer chain has occurred (cf. refs 6 and 10), which is clearly seen when structures **a** and **g** in Figure 2 are compared. Flipping of the polymer chain due to migratory insertion was postulated in the Cossee mechanism[6], but has, to our knowledge, not been explicitly supported by quantum chemical calculations earlier.

It is appropriate to question whether the use of SCF-optimized geometries can give reliable energy differences in transition metal systems like the present. As recently pointed out by Siegbahn and Svensson,[55] competing electron configurations, more likely to be a problem for first-row than second-row transition metal complexes, are the main reason why the SCF approximation may give unreliable geometries. Fortunately, this problem is easy to detect in a subsequent CI calculation. Our MCPF calculations revealed that the Hartree–Fock reference configuration is absolutely dominating for all the structures **1**–**5**, the largest coefficients of the competing configurations never exceeding 0.09. This clearly indicates that the accuracy seen for SCF geometry optimizations of second- and third-row transition metal complexes[32,33,60–65] also should be valid in our case. In ref 55, it is concluded that geometry optimization at the SCF level with double-ζ basis sets is sufficient when the final energy evaluation at the present level is performed.

In a recent paper by Weiss *et al.*,[20] inclusion of electron correlation in the geometry optimization is reported to be important for titanocene systems. Specifically, SCF theory did not predict the agostic reactant and product structures found with second-order Møller–Plesset (MP2) theory and LDA (local density approximation) theory for the insertion of ethylene in $Cp_2TiCH_3^+$. Furthermore, the π complex intermediate and the transition state of ethylene insertion which were located at the SCF level in ref 20 do not exist at the two correlated levels. Rather, the reaction was found to proceed below the reactant asymptote without passing any stationary point. However, it is interesting to note that the MP2 energies reported for the SCF-optimized geometries clearly indicate that the reaction proceeds downhill at the correlated level.

Weiss *et al.* also report MP2 geometry optimizations of the ethylene insertion in $Cl_2TiCH_3^+$. This part is of special relevance to the present work as $Cl_2TiCH_3^+$ may be considered to be the active part of our model. The MP2 energies reported are, relative to isolated reactants, −42.0, −39.5, and −57.9 kcal/mol for the π complex, transition state, and product, respectively. These energies may be compared to the MP2 energies evaluated in SCF-optimized geometries, as reported by Kawamura-Kuribayashi *et al.*[16] The latter values read −45.3, −41.0, and −56.4 kcal/mol. SCF- and MP2-optimized geometries thus seem to give very similar energetics for this reaction, and the rather small deviations may very well be the result of different basis sets. To check for the effects of dynamical electron correlation in the geometry optimizations of the present complexes, the structures **1** and **3** were reoptimized at the MP2 level.[66] This reduced the asymmetry in the chloride bridges somewhat and shortened the Ti(1)–C(2,3) distances by almost 0.3 Å but did not alter the lengthening of the C–C bond (~0.01 Å) in ethylene during complexation. The shorter titanium–ethylene distance in the MP2-optimized geometry suggests that the SCF approximation fails in the description of this weak dipole–induced dipole bond. However, the use of MP2-optimized geometries for **1** and **3** only increased the ethylene binding energy by 1 kcal/mol at the MCPF level, thus confirming the expectation that the use of SCF-optimized geometries only introduces minor errors in the present energy evaluations.

For further evaluation of the present SCF-optimized geometries, it is useful to compare some parts of the structures **1**–**5** with experimentally determined structural parameters for related compounds. The Ti(1)–Cl(5,6) distances, 2.22–2.32 Å, are in excellent agreement with X-ray diffraction data for terminal Ti–Cl bonds, 2.22–2.31 Å,[67] in titanium tetrachloride ester complexes. Furthermore, the calculated Ti–alkyl distances in **1**, **2**, **3**, and **5**, 2.04–2.05 Å, agree very well with the Ti–C distance of 2.042 Å found in electron diffraction studies of $TiCl_3$-CH_3.[68] The present calculated Al–H distances of 1.58 Å also seem to be reasonable as the two symmetry unique terminal Al–H bonds in $[Cp_2Ti(\mu\text{-}H)_2AlH_2](CH_3)_2NC_2H_4N(CH_3)_2C_6H_6$ have been reported to be 1.459 and 1.659 Å, respectively.[69] The structure was determined by X-ray diffraction.

3.2. The Energies of the Reaction. The SCF and PCI-80 energy profiles for the present reaction are shown in Figure 3. In Table 3, the energies and enthalpies at the important stationary points are given relative to the reactant asymptote, at the various levels of theory employed. The calculations show that, at the SCF level of theory, barriers for both ethylene coordination (4–6 kcal/mol) and insertion (23–24 kcal/mol) exist. Electron correlation makes the main features of the PES less pronounced. The barriers are lowered drastically and even eliminated when the most accurate method is employed. The resulting energy surface of the reaction is remarkably flat, and a large gain in energy is only obtained after the transition state of ethylene insertion.

The negligible small or nonexistent barriers calculated at correlated levels of theory indicate that the present reaction should be fast. During recent years, several authors have reported that the reaction proceeds below the reactant asymptote.[14–17,19–22] For these calculations, cationic models have been used, and the attractive charge-induced dipole force causes a large energy gain already in the step of olefin coordination to the metal. A small barrier to insertion from the π complex is found in most of the calculations, but the PES still runs far below the asymptote throughout the reaction.

Our rather flat PES running close below the asymptote from the start of the reaction to the transition state of the ethylene insertion (as located at the SCF level) represents a qualitatively different situation. Still, this result is expected and readily explained, as a neutral model reduces the affinity for the olefin and brings the first part of the PES much closer to the asymptote. Secondly, inclusion of correlation effects causes a favoring of

(60) Blomberg, M. R. A.; Siegbahn, P. E. M.; Svensson, M. *J. Am. Chem. Soc.* **1992**, *114*, 6095.
(61) Siegbahn, P. E. M. *Theor. Chim. Acta* **1993**, *86*, 219.
(62) Siegbahn, P. E. M.; Blomberg, M. R. A.; Svensson, M. *J. Am. Chem. Soc.* **1993**, *115*, 4191.
(63) Blomberg, M. R. A.; Siegbahn, P. E. M.; Svensson, M. *J. Phys. Chem.* **1993**, *97*, 2564.
(64) Bauschlicher, C. W., Jr.; Langhoff, S. R. *J. Phys. Chem.* **1991**, *95*, 2278.
(65) Rosi, M.; Bauschlicher, C. W., Jr. *Chem. Phys. Lett.* **1990**, *166*, 189.
(66) Jensen, V. R.; Børve, K. J.; Westberg, N.; Ystenes, M. *Organometallics*. Submitted.
(67) Rytter, E.; Kvisle, S.; Nirisen, Ø.; Ystenes, M.; Øye, H. A. In *Transition Metal Catalyzed Polymerizations: Ziegler-Natta and Metathesis Polymerizations*; Quirk, R., Ed.; Cambridge University Press: Cambridge, 1988; p 292.
(68) Berry, A.; Dawoodi, Z.; Derome, A. E.; Dickinson, J. M.; Downs, A. J.; Green, J. C.; Green, M. L. H.; Hare, P. M.; Payne, M. P.; Rankin, D. W. H.; Robertson, H. E. J. *J. Chem. Soc., Chem. Commun.* **1986**, 520.
(69) Lobkovskii, E. B.; Soloveichik, G. L.; Sisov, A. I.; Bulychev, B. M.; Gusev, A. I.; Kirillova, N. I. *J. Organomet. Chem.* **1984**, *265*, 167.

the structures in the molecular region (**2**–**5**) and especially the transition state of ethylene insertion (4). The present PES is also quite different from the results of Novaro *et al.*,[24,25] who used a neutral model quite similar to ours. Their calculations predicted a barrier of 19.2 kcal/mol to insertion from the π complex (15 kcal/mol above the reactant asymptote) and an overall reaction energy of −40.3 kcal/mol. The deviations are due to small basis sets, no correlation treatment, and assumed geometries in these more than 16 year old calculations.

Inclusion of HF limit corrections, zero-point vibrational effects, and temperature corrections (as described in the Computational Details section) to form the "best estimates" of the energy and enthalpy throughout the reaction is seen to favor the reactants. The corrections do not alter the fact that our calculated energies for the structures **1**–**4** are remarkably similar, the largest deviation in enthalpy from the reactants never exceeding 1 kcal/mol. On the basis of the accuracy reported for the PCI-80 method in ref 55 and our discussion of the reliability of SCF-optimized structures for the present system, the largest error is not expected to exceed 4 kcal/mol for the present calculated energy and enthalpy differences. It is encouraging that the calculated overall reaction enthalpy (−21.9 kcal/mol) is seen to compare very well with the experimental reaction enthalpy for gas-phase addition of ethylene to alkanes larger than methane (−22.2 kcal/mol, 298 K[31]). That this simple gas-phase reaction should compare with the catalytic reaction is based on the assumption that the strength of the metal–carbon bond broken and the metal–carbon bond formed is independent of the alkyl chain length, which seems to be reasonable.[32]

The experimentally reported activation energies are generally somewhat higher, 6–12 kcal/mol in refs 27–30, than the present estimate (−1.0 kcal/mol). Experimentally determined barriers may be increased by competing reactions, overlayed activation/deactivation reactions, and possibly also diffusion barriers. Theoretically estimated activation energies should therefore be equal to or lower than these. There is an ongoing discussion of how well the ion pair of the general type Cp_2MR^+ and $AlCl_4^-$ is separated during the catalytic process.[12] The model used by us is a "worst-case" situation, in that we have the smallest degree of separation between the two ions, which means that the present calculations should provide an upper bound for the PES of the reaction. The present estimated activation energy is still smaller than the experimental values, which suggests that the barrier measurements[27–30] do not correspond to the insertion step, as recently also suggested by Weiss *et al.*[20]

Theoretical investigation of ion pairs and the role of the cocatalyst should in the future be extended to include catalytically active metallocene systems. At the present stage, it should suffice to note that reasonable geometries have been reported[70,71] when modeling Cp by Cl in structures related to the present, as well as similar energy profiles for ethylene insertion.[16] Some differences, especially connected to agostic effects, have recently been reported by Weiss *et al.*[20] concerning ethylene insertion in $Cl_2TiCH_3^+$ and $Cp_2TiCH_3^+$.

A comparison of the populations in Table 4 to detailed studies of smaller models promoting olefin insertion into metal–carbon and metal–hydrogen bonds[22,32,33] may add to the understanding of the electronic effects present during the reaction. It is important to reduce the amount of repulsive nonbonding s,p electrons at the transition state of olefin insertion, which is accomplished by adding covalent ligands.[32,33] The electronegative chloride ligands present in our model obviously play this role, and especially a low s population (0.44–0.47 *e*) is noted throughout the reaction. Because of the high coordination number on the metal, a relatively large amount of valence p electrons is involved in metal–ligand bonds compared to the low coordinate Zr and Ti models in refs 22, 32, and 33, giving p populations of 0.6–0.7 *e* throughout. At the transition state of olefin insertion, the metal must form simultaneous bonds toward both the polymer chain and the monomer, and these bonds should be close to each other. The d orbitals are best suited for this task because of the small angle between the lobes,[22] and this is the reason why the d population is 0.1 *e* higher at the transition state than for the other structures.

Table 4. Mulliken Populations [*e*] for the Reactants (**1**), the Transition State of the π Complexation (**2**), the π Complex (**3**), the Transition State (**4**), and the Product (**5**) of Ethylene Insertion

population	1	2	3	4	5
Ti populations					
3d	2.28	2.26	2.26	2.38	2.28
4s	0.45	0.46	0.46	0.47	0.44
4p	0.57	0.61	0.63	0.68	0.58
atomic charges					
Ti	+0.60	+0.56	+0.54	+0.36	+0.59
C(2)	−0.43	−0.43	−0.43	−0.47	−0.54
C(3)	−0.43	−0.46	−0.46	−0.41	−0.33
C(4)	−0.77	−0.77	−0.77	−0.73	−0.66
Cl(5)	−0.16	−0.22	−0.23	−0.25	−0.18
Cl(7)	−0.40	−0.35	−0.36	−0.44	−0.48
Cl(8)	−0.46	−0.50	−0.50	−0.44	−0.40
AlH_2Cl_2[a]	−0.34	−0.34	−0.34	−0.38	−0.36
H(12)	+0.22	+0.26	+0.27	+0.31	+0.27
H(14)	+0.22	+0.25	+0.26	+0.30	+0.23
H(16)	+0.28	+0.29	+0.29	+0.29	+0.23
H(18)	+0.28	+0.27	+0.27	+0.30	+0.23

[a] The total charge on the aluminum moiety.

The negative charge on the aluminum moiety (AlH_2Cl_2, ~−0.35 *e*) is almost constant during the reaction, suggesting that a main role is to provide a partial ionization of the titanium moiety and to induce a certain degree of rigidity in the structure, in accordance with suggestions in ref 72. However, the large differences seen in the bridging bonds during the reaction probably also participate in relaxing the structure and damping the energy variations. At the transition state, when the metal is forming bonds toward the polymer chain and the monomer, it should be an advantage that the *trans* ligands are not too strongly bound. This seems to be the case in the present model, as the two Ti–Cl bridging bonds are both relatively long (~2.6 Å) at the transition state, and in fact, the sum of the overlap populations for these two bonds is lower at the transition state than for the rest of the complexes, as seen in Table 2.

The apparent effect of geometrical relaxation in the chloride bridges during the ethylene insertion process is interesting as such bridges are expected to exist in heterogeneous $TiCl_3$-based or $MgCl_2$-supported catalysts. The charges calculated for the chloride bridges, ~−0.5 *e*, are significantly more negative than for the terminal chlorides, ~−0.2 *e*, thus being closer to what is expected for chlorides present at a polar or ionic surface. It is desirable to check if the main features of the investigated model is present when the active center is bridged to the support. A study of this type of center, with $MgCl_2$ as the support, is in progress.

4. Conclusions

The direct Ziegler–Natta ethylene insertion into the titanium–methyl bond in the neutral, bimetallic $AlH_2(\mu\text{-}Cl)_2TiCl_2(CH_3)$

(70) Upton, T. H.; Rappé, A. K. *J. Am. Chem. Soc.* **1985**, *107*, 1206.
(71) Koga, N.; Morokuma, K. *J. Am. Chem. Soc.* **1988**, *110*, 108.
(72) Jensen, V. R.; Ystenes, M.; Wärnmark, K.; Åkermark, B.; Svensson, M.; Siegbahn, P. E. M.; Blomberg, M. R. A. *Organometallics* **1994**, *13*, 282.

has been studied using analytic gradient methods in the geometry optimizations and reaction pathway calculations. Effects of electron correlation have been included at the important stationary points along the reaction path. No barrier was found for either the ethylene coordination or the insertion at the correlated level, and the PES runs close below the asymptote from the reactants to the midpoint of ethylene insertion (the SCF-optimized transition state). Only after this point is a large gain in energy obtained. The reason why the PES is relatively flat through the first part is mainly that the present neutral model does not exert a large attraction on the olefin. The chloride bridging bonds seem to be important for the current migratory insertion as they are positioned *trans* to the polymer and the ethylene at the transition state of olefin insertion. The bond distances vary substantially (~0.4 Å) during the reaction, synchronously with the polymer chain flipping. In addition to the *trans* influence from the chloride bridges and the rigidity following these, the cocatalyst "counterion" performs a partial ionization. The aluminum moiety, AlH_2Cl_2, has a Mulliken charge of ~ -0.35 *e* throughout the reaction.

Even if our worst-case error estimate of 4 kcal/mol is added to the barrier, this still gives an activation energy of ethylene insertion below the experimental values. This suggests that the reported experimental activation energies may be influenced by competing reactions or diffusion barriers. Separation of the catalyst ion pair does not seem to be necessary for obtaining a viable insertion reaction, but increasing the charge separation will tend to favor both the coordination and insertion step as compared to the present results.

Acknowledgment. A scholarship from the Norwegian Institute of Technology is gratefully acknowledged (V.R.J.), as is financial support from The Norwegian Academy of Science and Letters and Den norske stats oljeselskap a.s. (VISTA, grant no. V6415) and a grant of computing time from the Norwegian Supercomputing Committee (TRU). The authors also want to thank Intel Corporation for support through the SINTEF/Intel Paragon Supercomputer Partnership Agreement. In addition to this, V.R.J. appreciates additional funding from Anders Jahres Fond. Profs. Björn Åkermark and Per E. M. Siegbahn, Drs. Mats Svensson, Kenneth Wärnmark, and Margareta R. A. Blomberg are thanked for interesting discussions regarding the Ziegler–Natta process. Prof. Donald G. Truhlar and an anonymous referee are thanked for valuable comments concerning the bifurcations of our reaction path. Finally, we are indebted to Mr. Bjarne G. Herland at Parallab, University of Bergen, for help with software on Intel Paragon and visualization of the reaction path.

Supplementary Material. Pictures of the present model system, as well as a movie consisting of every fifth point located on the reaction path, are available on World Wide Web (http://www.ii.uib.no/plab/VIZ/index.html).

JA942401I